Fracture Mechanics of Concrete and Concrete Structures - High Performance, Fiber Reinforced Concrete, Special Loadings and Structural Applications- B. H. Oh, et al. (eds)

Cracking analysis of brick masonry arch bridge

J. M. Chandra Kishen & Ananth Ramaswamy
Dept. of Civil Engineering, Indian Institute of Science, Bangalore 560012, India

ABSTRACT: In this work, details of field measurements undertaken at a brick masonry arch bridge under design train traffic and analytical work based on non-linear fracture mechanics are presented. A parametric study is done to study the effects of tensile strength on the progress of cracking in the arch. Further, a stability analysis to assess collapse of the arch due to lateral movement at the springing, in particular near the partially filled land arches is done. The margin of safety with respect to cracking and stability failure is computed. Conclusions are drawn on the overall safety of the bridge.

1 INTRODUCTION

Most of the railway bridges in the Indian Railway system that have been built several decades ago have deteriorated both in terms of strength and stiffness due to a variety of reasons. These bridges have been designed for live loads and service conditions that have changed drastically with time. Increased axle loads and traffic density have necessitated bridge owners to get the bridge condition assessed in order to determine their residual structural strength and identify strengthening measures to be taken for safe performance.

Condition assessment provides information regarding the intensity and extent of observed defects, the cause for these defects and possible deterioration processes that have strong impact on the safety and service life of structures. Furthermore, this information forms the basis for estimating the residual structural capacity and possible remedial work that needs to be undertaken.

The present study focuses on a brick masonry arch bridge in the South Western Railway zone of the Indian Railways. The bridge has been constructed with brick masonry with possibly a compacted granular soil infill and dates back to the 1870's when it was part of a meter gauge line. Over the years, the passenger and freight traffic have increased on this section and the section has been transformed through a gauge conversion to broad gauge traffic. The permitted axle load untill a few years ago was classified as 18t axle load and has subsequently undergone an upward revision to 22t axle based on an in-house assessment undertaken by the Indian Railways. At present, there has been a growth in freight traffic in this section, in particular for iron ore and coal movement, and the Indian Railways is considering the possibility of further enhancing the permitted axle load to 25t immediately with possible further upward revisions at a later date.

The condition assessment of the bridges in this section has been initiated with a view to understand the present state of the bridge and the ramifications of increasing the payload on the bridge with or without any intervention for structural enhancement. In this paper, details of field measurements undertaken at the bridge under design train traffic and fracture mechanics based finite element analysis are presented. Conclusions are drawn with some remarks on the state of the bridge within the framework of the information available and inferred.

2 DETAILS OF BRIDGE

The bridge considered in this study is a brick masonry arch bridge built in the 1870's on a meter gauge section. The bridge consists of two major arches across a water fall with spans of 17.7m and 17.3m (Fig. 1) at springing level and a few smaller arches of approximately 7.7m that are land arches and partially closed. The carriage width of the bridge is 8.8m and is slightly curved in plan and has a steep rising gradient of 1 in 30. The railway line alignment is eccentric with respect to the bridge centerline. The arch has a central rise of about 4.5 meters. The rings of the arch are about 0.93m in thickness across the arch barrel, with a brick masonry facing on either side rising up to the top of the bridge with a parapet of a meter height on either side. The abutments and piers appear to consist of brick masonry that has been encased in reinforced concrete during an earlier intervention. The piers and abutments rest on bed rock. The pier width is about 3.82m at the base and varies over the height. Figure 1 shows the schematic sketch of the bridge.

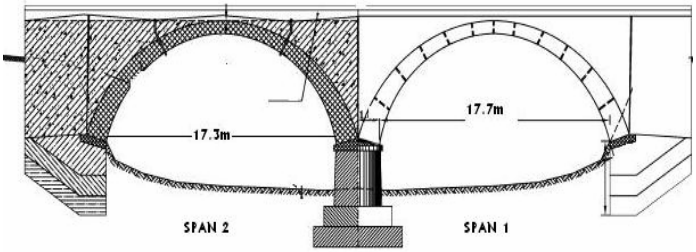

Figure 1. Schematic sketch of brick masonry arch bridge. (Left end: Kulem (K) end; Right end: Castle Rock (CR) end).

3 INSTRUMENTATION

A 64 channel data acquisition system (M/s Dewetron, Austria) was used for acquiring the data continuously from all the sensors. The sensors used with this acquisition system consisted of linear variable differential transformer (LVDT) to measure displacements, namely, vertical crown displacements and horizontal springing displacements; electrical resistance strain gauges to measure surface strains in a particular direction, either along the circumferential direction of the arch or the arch barrel at the crown, quarter and three quarter point and springing levels and on the rails; vibrating wire strain gauges mounted on the arch and parapet; uniaxial and tri-axial accelerometers to measure the acceleration levels in terms of 'g' levels at the track level (sleepers) and corresponding locations on the arch surface. A temperature sensor was fixed on the bridge to measure the variations in the temperature. A tilt sensor was placed on the vertical surface of the pier. The LVDTs were located on the arch surface and strain gauges were located on the arch intrados, parapet and rail.

4 LOADING SCHEMES

A series of four major loading tests: static load tests; quasi-static moving load tests; speed tests and longitudinal load tests were carried out over a four-day period. In this study, only the first two tests are used and hence are described in detail.

Static Load Test: Two BRN wagons whose axles spacings are shown in Figure 2 and loaded with 200 (approx. 20.75 T axle load), 184, 168 and 152 prestressed concrete sleepers were placed on the bridge structure at a fixed position. The two wagons could apply a static load on both the spans of the bridge. Displacements and strains were measured at various locations on the bridge for each load level of this test.

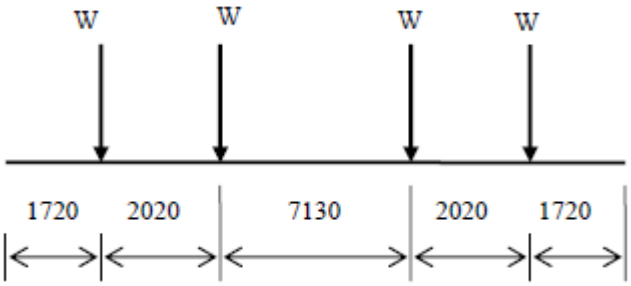

Figure 2. Spacing of axles in BFR wagon.

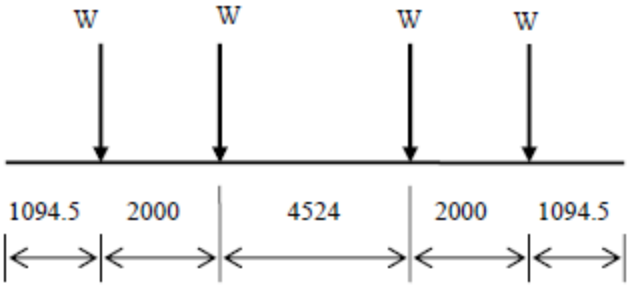

Figure 3. Spacing of axles in BOXNEL wagon.

Quasi-static Moving Load Test : A train formation consisting of two locomotive engines (WDG4), two BFR wagons with 152 sleepers in each, two goods wagon filled with 25 t axle load with four axles each (BOXNEL whose axle spacing are shown in Figure 3), followed by two locomotive engines (WDG3A), was positioned on the bridge at different predetermined locations and measurements were taken. At the start of the test, the first wheel of WDG4 wagon was placed on the left springing position of span 1. The test progressed with subsequent wheels of the formation occupying this first reference point is succession. Since the formation had forty wheels, the same number of measurements was taken. This test was performed to obtain the variations in deflections and strains for different positions of the load. Such variations are typically determined in computational models using the well known method of influence lines.

5 RESULTS OF FIELD TESTS

In this section, the results of the various field tests conducted on the arch bridge as indicated in Section 4 have been presented.

5.1 *Results of static tests*

Table 1. Vertical deflections at the crown.

Load	Span 1 mm	Span 2 mm
168 sleepers	0.49	0.30
184 sleepers	0.55	0.60
200 sleepers	0.57	0.60

The static response in terms of vertical deflection at the crown central position is shown in Table 1. The observed differences in the displacements of the two spans are indicative of the mild asymmetric nature that exists in the arch geometry.

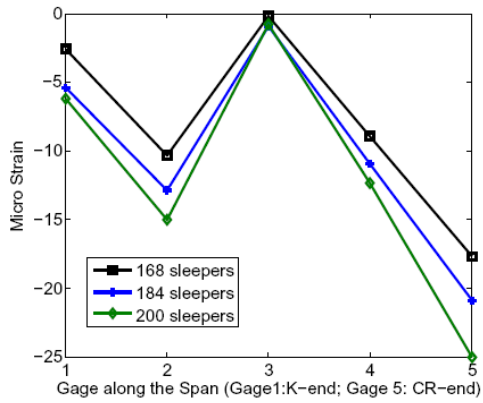

Figure 4. Tangential strains along the rail centerline.

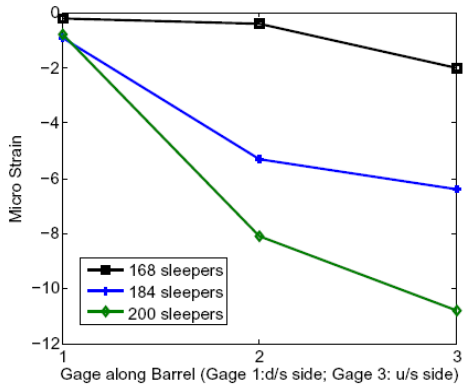

Figure 5.Tangential strain along the barrel of Span 1.

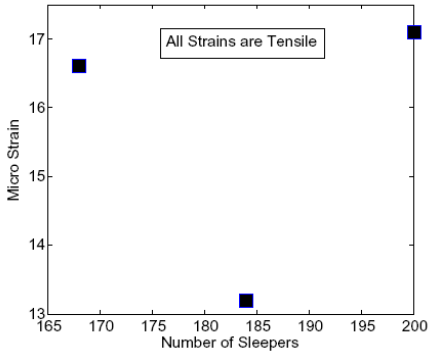

Figure 6. Transverse strains at crown of Span 1 for different magnitude of loads.

The tangential strains in span 1 along the centerline of the track are shown in Figure 4. The strains are minimum and almost zero near the crown and maximum near the right springing position. Figure 5 shows the tangential strains along the width of the arch at the crown position. It may be mentioned here that one micro strain corresponds to approximately 0.0018 MPa (0.018 kg/mm^2) of stress in the masonry. It is seen that the strains are largest near the eccentric position (far end of the barrel of arch) when compared to the centre line of rail location.

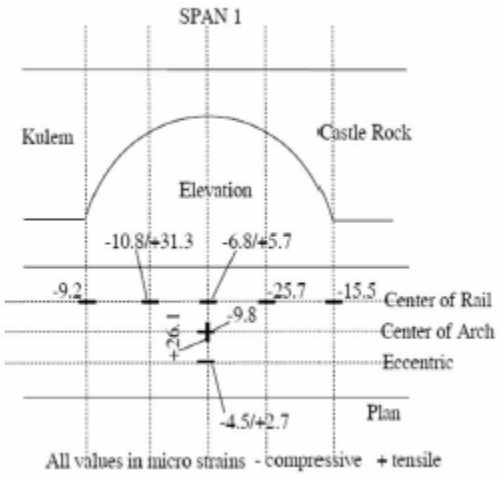

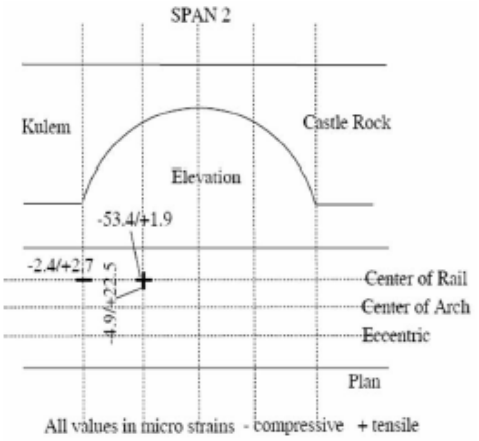

Figure 7. Maximum strains measured in Span 1 and Span 2 during the quasi-static test.

Figure 6 shows the transverse strains along the crown for different magnitude of loading. It is seen that all the transverse strains are tensile in nature. The maximum value of transverse tensile strain is about 17 microstrains which corresponds to a tensile stress of about 0.00306 kg/mm^2. This value is less than the codal permissible value [Code A, Rule A] of 0.011 kg/mm^2 in tension.

5.2 *Results of quasi-static moving load test*

The influence line like study indicates that the maximum vertical displacement on the crown is about 0.88 mm and the maximum horizontal springing deflection is 0.1mm at abutment and 0.17 mm in the central pier in span 1. In span 2 the maximum vertical deflection at the crown is 0.75 mm, while the springing deflection in the abutment was 0.01mm and -1.4mm / +1.2mm in the central pier due to a 25 t axle load. The negative value implies horizontal movement of the central pier to the left (Kulem side, Fig. 1) and the positive value represents horizontal movement towards Castle Rock side (Fig. 1). It may be mentioned here that the LVDT was mounted on the repaired (encased) concrete at the springing level. The large values of horizontal deflection suggests that delamination (separation) of the repaired concrete from the parent masonry pier could have occurred.

Figure 7 shows the maximum compressive and tensile strains measured at different locations on the bridge. The maximum value of strain is reckoned across the measured responses taken for all forty placements of the formation on the bridge.

6 FINITE ELEMENT ANALYSIS

In this section, details of finite element modeling of the arch bridge under various loading conditions have been presented. The analysis is done using the finite element program ATENA (Cervenka & Pukl, 2007). The Atena software has been used to study the bridge under monotonically increasing loads positioned as in rail load configurations with a view to understand cracking in masonry and its propagation. Furthermore, parametric studies have been undertaken by considering the tensile strength of brick masonry and filler and the boundary conditions as parameters.

The masonry arch bridge with a soil infill has been idealized as composed of two isotropic homogeneous materials, namely, masonry and filler. A two dimensional plane stress model of the bridge has been used in this study. The finite element package ATENA encompasses many material model formulations for quasi-brittle concrete like materials, such as a bi-axial failure surface with different tension and compression thresholds, post crack strain softening based on exponential and multi-linear softening, specific fracture energy of the material, compression softening in cracked concrete and other fracture based parameters, such as crack interface shear transfer.

A two-dimensional plane stress finite element model for the masonry arch bridge is shown in Figure 8. The brick masonry has been assumed to have a modulus of 1800 MPa and a Poisson's ratio of 0.2. The soil infill has been idealized to have modulus of 800 MPa with a Poisson's ratio of 0.18. A relatively small tensile strength of 0.3 MPa has been assumed for the masonry with a similar value of 0.3 MPa for the infill. These values are obtained through an iterative process of model calibration using the field measurements of the static load – deflection and quasi-static moving load studies. The boundary condition on the vertical face of the abutment (left end of span 2) is restrained in the longitudinal traffic direction and the base of the abutments and central pier have been constrained in the vertical direction. The boundary at the right side abutment of span 1 has been elastically constrained for longitudinal movement using linear springs (the value of this spring constant is reported later).

The following studies have been undertaken:

1. Simulation of static load – deflection test (BFR wagons carrying PSC sleepers positioned as in the field studies).
2. Simulation of quasi-static moving load test (25 t axle load BOXNEL wagons arranged at critical position as in the field studies)
3. Parametric studies varying tensile strength of brick masonry and filler and the boundary condition of the abutment of span 1 on the Castle Rock end. It may be recalled that a few smaller land arches of approximately 7.7m span are present on the Castle Rock end of Span 1 that are partially closed. Hence, this boundary is simulated by providing springs and also by restraining it completely.

6.1 *Simulation of static load test*

In this study, the two BFR wagons with PSC sleepers (as detailed above) are placed on the bridge with loads coinciding with the axle position as in the field test.

The vertical deflection obtained at the crown of span 1 is 0.55 mm as against a measured value of 0.57 mm for BFR with 200 sleepers. The corresponding value of computed and measured vertical deflection at the crown of span 2 is 0.54 mm and 0.6 mm. This indicates that the material properties of modulus of elasticity and Poisson's ratio used for the masonry and the infill in the analysis are in agreement with the deformations observed at field, thereby calibrating the material model.

6.2 *Simulation of quasi-static moving load test*

In this study, the entire rake used for this test as described above is used for applying the load on the

bridge in a sequential way. One particular position of the rake on the bridge which causes maximum effects has been simulated. Figures 8 and 9, show the finite element model and load positions, respectively.

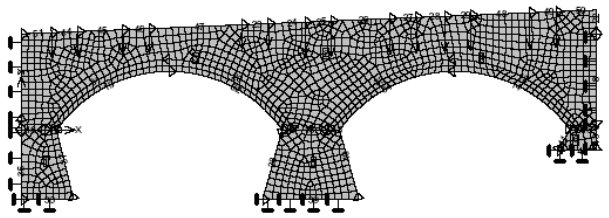

Figure 8. Finite element model with boundary conditions.

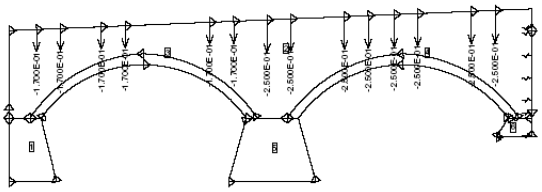

Figure 9. Loads on the finite element model.

Table 2 shows the results of this simulation at various points together with the field results for the loading configuration as in Figure 9. This loading configuration corresponds to one of an episode of the quasi-static load test that results in the highest crown vertical displacement.

Table 2. Results of finite element analysis.

Description	Span 1	Span 2
Crown displacements		
Computed (mm)	0.64	0.3
Measured (mm)	0.68	0.2
Crown strains		
Computed (microstrain)	10.7	1.26
Measured (microstrain)	8.35	Not measured

6.3 *Parametric study*

In the parametric study, the loading configuration used in the quasi-static test and shown in Figure 4.3 is considered. The tensile strength of the brick masonry and the filler and the boundary condition at the abutment of span 1 has been varied to study their influence on the crack widths and the failure mode.

No Cracking Analysis

The finite element analyses are done by assuming higher values of tensile strength of the brick masonry and the filler material in such a way that no cracks are developed when the axle load due to the BOXNEL reaches to about 105 t. The load configuration used is the same as shown in Figure 9. In the analysis the axle loads on the BOXNEL wagons are increased in steps of 5 t from an initial value of 25 t. The corresponding loads of the 168 sleepers loaded BRN wagons are scaled up proportionately. The boundary of the abutment of span 1 on the Castle Rock end (Fig. 1) is assumed to be on springs. The spring constant (1300 N/mm) is calibrated such that for an axle load of 25 t on the BOXNEL wagons, the deflection at the crown of spans 1 and 2 match with the field measurements.

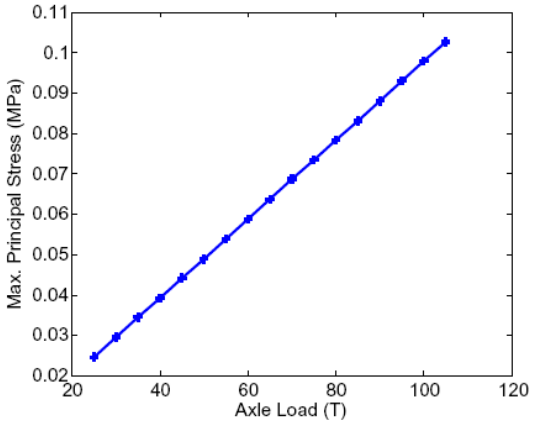

Figure 10. Maximum Principal Stress (without self weight) versus Axle Load at Crown of Span 1.

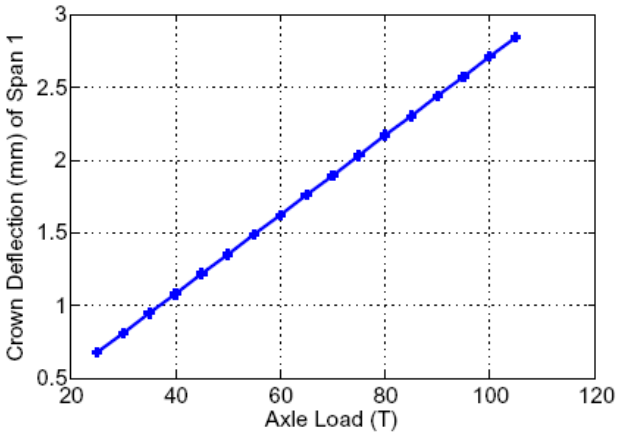

Figure 11. Vertical Deflection at Crown of Span 1 versus Axle Load.

Figure 10 shows the plot of maximum principal stress at the crown of Span 1 with respect to the applied axle load. From this figure, it is seen that the rise in the maximum principal stress is only about 0.1 MPa for an increase of 100 t axle load which is quite small. Furthermore, at 25 t axle load and without the self weight, the maximum principal stress near the crown is 0.0245 MPa (0.16 MPa with self weight). Since no cracking was observed at this load in the field studies, it is expected that the minimum

tensile strength of the masonry arch is over 0.16MPa.

Figure 11 shows the vertical deflection at the crown of span 1 with the self weight and increasing live load. The live load corresponding to a relative displacement of 1.2 mm (Code A) caused by live load alone is 45 t. This corresponds to a margin of safety at 25 t equal to 1.8. This margin of safety is over and above the margin already provided by the code. For completeness, the vertical crown deflection of Span 2 are also computed and are found to be lower than those in Span 1 since this part of the span is subjected to loads lower than those in Span 1.

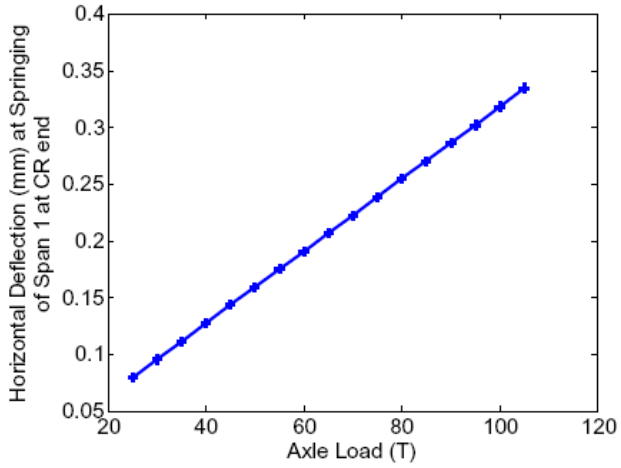

Figure 12. Horizontal Deflection at Springing of Span 1 (CR-end) versus Axle Load.

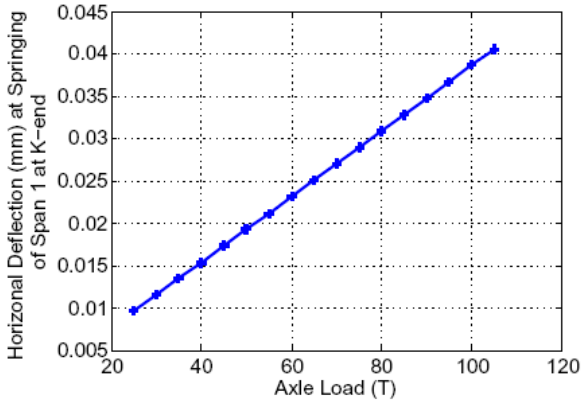

Figure 13. Horizontal Deflection at Springing of Span 1 (K-end) versus Axle Load.

Figures 12 to 15 show the horizontal deflection at the springing of abutment and piers of span 1 and span 2 respectively with increasing axle load.

From Figure 12 it is seen that for a relative displacement (i.e., due to live load alone) of 0.2 mm (Code A) at the springing the corresponding live load is 65 t. This offers a margin of safety at 25 t axle load of 2.6 over and above the margin offered by the code itself. The horizontal deflection observed at other springing (Figs. 13 – 15) is less than 0.2 mm for an axle load of 105 t.

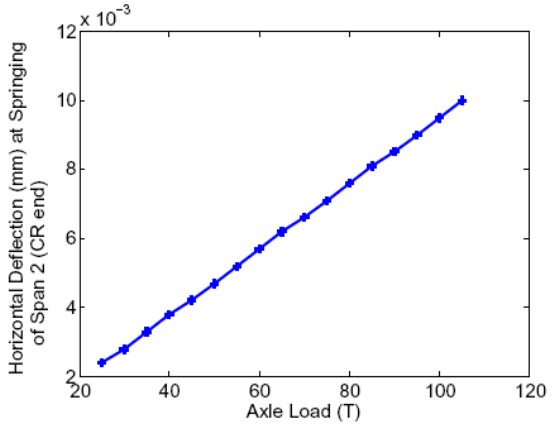

Figure 14. Horizontal Deflection at Springing of Span 2 (CR-end) versus Axle Load.

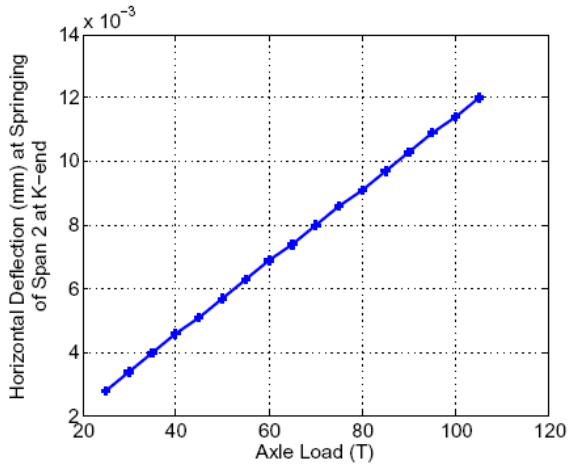

Figure 15. Horizontal Deflection at Springing of Span 2 (K-end) versus Axle Load.

Cracking analysis

A cracking analysis is carried out to determine if the failure of the arch bridge takes place due to excessive cracking near the crown or by any other mode. The tensile strength of brick masonry of 0.20 MPa is used and the analysis is carried out by applying the self weight and incrementally increasing the axle loads on the BOXNEL wagons in steps of 5 t. The corresponding loads of the 168 sleepers loaded BRN wagons are scaled up proportionately. It was found that the crown starts to crack at an axle load of 15 t. The cracking process continues and at an axle load of 40 t the crack reaches the entire thickness of the brick arch. The crack widths from this incremental analysis is plotted against the axle load in Figure 16. It is seen that the crack widths increase at a faster rate after 40t axle load that is when the crack has

propagated through the entire thickness of the brick arch. Thereafter, on increasing the axle load the crack width increases without the crack propagating further. The arch softens considerable due to increased opening of the crack. The final failure may take place due to cracking at the crown of the arch.

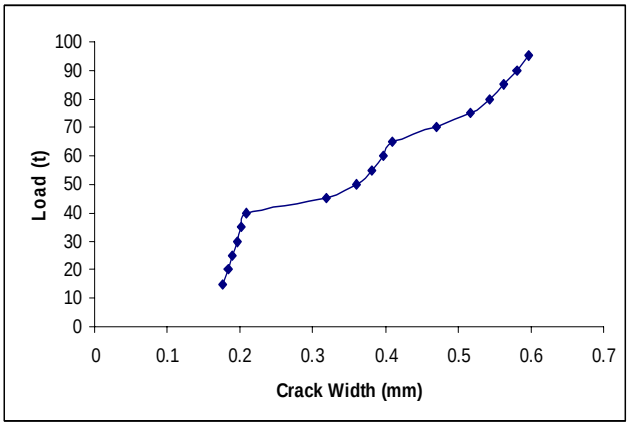

Figure 16. Crack width versus axle load at crown of Span 1.

6.4 *Analysis with tractive forces due to braking*

A longitudinal tractive force analysis is carried out by including horizontal forces at the rail level at wheel position equal to about 35 t based on an average field measured value. For this analysis, a tensile strength of 0.2 MPa is assumed for both the brick masonry and the filler material. From this analysis, it was observed that cracking initiated at the crown of Span 1 at a live load of 65 t, offering a margin of safety of 2.6 with respect to a 25 t axle load. Furthermore, no cracks were observed at the springing of the pier and abutments, suggesting that the hinging mode of failure is unlikely. It may be noted here that the failure of the arch through the formation of hinge near the crown can take place if there is excessive horizontal movement at the springing of the abutment.

7 ESTIMATION OF FATIGUE LIFE

The bridge structure is subjected to repeated fluctuating loads due to the passage of trains. The loss of mechanical integrity of the structure due to this repeated fluctuating load is known as fatigue. A component which fails at a high constant load, may fail under a substantially smaller fatigue load. The process of fatigue in the masonry arch bridge may lead to excessive deformations, formation of tension zones at the crown region of the arch and cracking of mortar in the masonry.

It may be mentioned here that a small tensile stress is observed in the static analysis of the arch bridge. This may not be the case when the bridge is newly constructed and is at its beginning of service life. Due to repeated loading over a period of time (about 120 years), stiffness degradation and damage accumulation could have taken place and hence the major principal stress near the crown region is inferred to be tensile.

Empirical relations are developed, especially for metals, that relate the applied stress (peak value of the fluctuating load) and the number of cycles N required to cause the failure. This relation is generally known as the $S - N$ curve. The major drawback of the $S - N$ curve approach is that it does not explore the mechanisms of failure and it does not distinguish between crack initiation life and crack propagation life, only the overall fatigue life is considered. Furthermore, in this approach, there is hardly any consideration on size effects: that is, data generated on small size specimen in a laboratory is directly applied on large size components. Also, the data on $S - N$ curve has a large scatter suggesting that the formulation needs to be more rigorous. To overcome these drawbacks of the $S - N$ curve approach, more sophisticated models are developed using the concepts of fracture mechanics. In this theory of fracture mechanics, a crack is assumed to exist at the position where maximum tensile stress occurs. The rate of propagation of this crack with respect to the number of cycles of fatigue load is computed and this defines the fatigue life of the component / structure.

The simplest crack propagation law is the Paris law which is defined by [Kumar 1999]

$$\frac{da}{dN} = C\,(\Delta K)^m \tag{1}$$

where a is the crack length, N is the number of cycles of fatigue load, (ΔK) is the stress intensity factor range, C and m are material constants.

The fatigue life estimation for the arch bridge is done using the above Paris law. The material parameters for mortar used in the present case for masonry are assumed as C = 1.70E-03 m/cycle and m = 2.1.

The stress intensity factor range is computed as [Kumar 1999]

$$\Delta K = f(\beta)\,\Delta\sigma\sqrt{\pi a} \tag{2}$$

where $\Delta\sigma$ is the stress amplitude range = $\sigma_{max} - \sigma_{min}$. This is considered to be equal to 0.06 MPa which is the difference of the maximum and minimum principal stress as obtained in the analysis using the 25 t axle load. The factor $f(\beta)$ is the geometry factor = 1.3 for circular arch. An initial crack size of 0.1 mm is assumed at the crown of the arch.

Numerical integration is performed on the Paris law and the number of cycles required for an initial crack of size 0.1 mm to propagate until the crack grows to a size of 10 mm is obtained as 242.6E+03 cycles. Assuming each cycle of loading to be a passage of train (54 Wagons + 7 WDG4) loaded to 25 t per axle, and assuming ten trains running on this bridge per day, it takes about 66 years for a crack of size 0.1mm to reach a size of 10 mm.

It may be noted that a crack initiated at the crown of the arch may propagate until half the ring thickness of the brick masonry which is 465 mm. Thereafter, this crack does not propagate further as due to stress redistribution, the nature of stress would be compressive. A compressive stress near a crack tip tends to close a crack and prevent further propagation. Hence, it is unlikely that the arch ring may collapse due to crack propagation. The cracking process may only result in excessive displacements and so these cracks have to be sealed during the regular maintenance program.

8 CONCLUSIONS

Based on the investigations, the following conclusions are made:

(1) From Field Measurements

- Under known loads (load deformation and quasi static load tests) the structural load deformational behavior is within the elastic regime based on the full recovery of the strains observed in the test. The stiffness properties used in the analytical simulations have been obtained from these tests.
- In the field measurements, it was observed that there were no visible cracks observed in the brick masonry under the applied axle load of 25t.
- The maximum stresses in the static and quasi-static tests are within the code permissible limits.
- The maximum displacements observed in the quasi-static tests indicate that they are within code permissible limits except for the springing displacement of the pier in Span 2. This may be due to the delamination caused between the outer concrete repair and the inner masonry pier.

(2) From Finite Element Analysis:

- Based on the IRS codal provisions on the displacements for Arch bridges, a margin of safety of 2.6 on crown displacements for a 25 t axle load is obtained over and above the margin provided by the code.
- Based on the IRS codal provisions on the displacements for Arch bridges, a margin of safety of 2.6 on springing displacements for a 25 t axle load is obtained over and above the margin provided by the code.
- The above margin of safety values drop to 2.6 for 25 t axle load over and above the margin provided by the code under the presence of longitudinal tractive forces (42 t) due to braking.

(3) From Fatigue Analysis:

- The estimated number of years for a crack at the crown of size 0.1 mm to grow to 10 mm assuming ten trains (54 wagons+7 WDG4) per day loaded to 25 t /axle pass on the bridge is 66 years.

9 ACKNOWLEDGEMENT

The financial support provided by the South Western Railway of the Indian Railways is gratefully acknowledged.

REFERENCES

Cervenka V. & Pukl R., 2007, ATENA program Documentation, Cervenka Consulting, Czech Republic, Praha.

Code A: Code of practice for the design and construction of masonry and plain concrete arch bridges (Arch Bridge Code), RDSO, Lucknow, India.

Kumar P, 1999.Elements of Fracture Mechanics, Wheeler Publishing, New Delhi.

Rule A: Rules specifying the loads for design of superstructure and sub-structure of bridges (Bridge Rules), RDSO, Lucknow, India.